Kekwick, R. A., & Cannan, R. A. (1936) *Biochem. J. 30*, 227.
Kornfeld, S., Li, E., & Tabas, I. (1978) *J. Biol. Chem. 253*, 7771.
Lee, Y. C., & Montgomery, R. (1962) *Arch. Biochem. Biophys. 97*, 9.
Levvy, G. A., Conchie, J., & Hay, A. J. (1966) *Biochim. Biophys. Acta 130*, 150.
Maizel, J. V., Jr. (1970) *Methods Virol. 5*, 179.
Muramatsu, T., Koide, N., Ceccarini, C., & Atkinson, P. H. (1976) *J. Biol. Chem. 251*, 4876.
Narasimhan, S., Harpaz, N., Longmore, G., Carver, J. P., Grey, A. A., & Schachter, H. (1980) *J. Biol. Chem. 255*, 4876.
Neuberger, A. (1938) *Biochem. J. 32*, 1435.
Nuenke, R. H., & Cunningham, L. W. (1961) *J. Biol. Chem. 236*, 2452.
Shepperd, V., & Montgomery, R. (1978) *Carbohydr. Res. 61*, 147.
Spiro, R. G., Spiro, J. J., & Bhoyroo, V. D. (1979) *J. Biol. Chem. 254*, 7659.
Stanley, P., & Sudo, T. (1981) *Cell (Cambridge, Mass.) 23*, 763.
Strecker, G., Herlant-Peers, M. C., Fournet, B., Montreuil, J., Dorland, L., Haverkamp, J., Vliegenthart, J. F. G., & Farriaux, J. P. (1977) *Eur. J. Biochem. 81*, 165.
Strecker, G., Fournet, B., & Montreuil, J. (1978) *Biochimie 60*, 725.
Tai, T., Yamashita, K., Ogata, M., Arakawa, N., Koide, N., Muramatsu, T., Iwashita, S., Inoue, Y., & Kobata, A. (1975) *J. Biol. Chem. 250*, 8569.
Tai, T., Yamashita, K., Ito, S., & Kobata, A. (1977) *J. Biol. Chem. 252*, 6687.
Tarentino, A. L., & Maley, F. (1974) *J. Biol. Chem. 249*, 811.
van Halbeek, H., Dorland, L., Vliegenthart, J. F. G., Schmid, K., Montreuil, J., Fournet, B., & Hull, W. E. (1980) *Eur. J. Biochem. 114*, 11.
Wolfe, L., Senior, R. G., & Ng Ying Kin, N. M. K. (1974) *J. Biol. Chem. 249*, 1828.
Yamashita, K., Tachibana, Y., & Kobata, A. (1978) *J. Biol. Chem. 253*, 3862.

Comparative Study of Ribonucleotide, Deoxyribonucleotide, and Hybrid Oligonucleotide Helices by Nuclear Magnetic Resonance†

Arthur Pardi,* Francis H. Martin,‡ and Ignacio Tinoco, Jr.

ABSTRACT: The nonexchangeable base protons and the hydrogen-bonding NH–N imino protons were used to study the conformations and the helix–coil transitions in the following oligonucleotides: (I) $dCT_5G + dCA_5G$, (II) $rCU_5G + rCA_5G$, (III) $dCT_5G + rCA_5G$, (IV) $rCU_5G + dCA_5G$. The first three mixtures all form stable double-helical structures at 5 °C, whereas IV forms a triple strand with an rCU_5G:dCA_5G 2:1 ratio. The chemical shifts of the imino protons in the double strands indicate that I, II, and III have different conformations in solution. For example, the hydrogen-bonded proton of one of the C·G base pairs is more deshielded (a 0.4-ppm downfield shift) in helix I than in helix II or III. This implies a significant change in helical parameters, such as the winding angle, the distance between base pairs, or overlap of the bases. The coupling constants of the H1′ sugar protons show that helix I has 90% 2′-endo sugar conformation, whereas helix III has greater than 85% 3′-endo conformation for the observed sugar rings. The sugar pucker data are consistent with helix I having B-family geometry; III has A-family geometry. The chemical shifts of the nonexchangeable base protons in system I were followed with increasing temperature. The midpoints for the transitions, T_m's, for all the base protons were 28–30 °C; this indicates an all-or-none transition.

Proton nuclear magnetic resonance (NMR)[1] studies of oligonucleotides have greatly increased our understanding of the conformations and physical properties of nucleic acids in solution. The chemical shifts of the NH–N imino resonances, base proton resonances, and the H1′ ribose or deoxyribose resonances have been used, separately or in combination, to deduce RNA A or A′ (Arnott et al., 1975) type conformations for double-helical ribooligonucleotides (Arter et al., 1974; Heller et al., 1974; Borer et al., 1975; Hughes et al., 1978). Double-stranded deoxyribooligonucleotides have shown spectra consistent with a B-form geometry in solution (Cross & Crothers, 1971; Patel, 1974; Kallenbach et al., 1976; Early et al., 1977). These conclusions are based mainly upon comparison of the experimental chemical shifts with those computed from ring current effects for an assumed geometry, as well as the sugar pucker deduced from the H1′ proton coupling constants.

X-ray studies of RNA–DNA hybrid duplexes have shown them to adopt A-type geometries (Milman et al., 1967; Arnott et al., 1975). The only ^1H NMR study of an RNA–DNA duplex shows the structure of the hybrid to be different than that of the DNA–DNA duplex of the same sequence and consistent with an A form in solution (Selsing et al., 1978).

Triple-stranded structures are not uncommon in polynucleotide or oligonucleotide solutions (Bloomfield et al., 1974). Under conditions where triplexes were formed, Geerdes

† From the Department of Chemistry and Laboratory of Chemical Biodynamics, University of California, Berkeley, Berkeley, California 94720. *Received November 21, 1980.* This work was supported by National Institutes of Health Grant GM 10840 and by the Division of Biomedical and Environmental Research of the Department of Energy under Contract No. W-7405-ENG-48. We also thank the Stanford Magnetic Resonance Laboratory (supported by National Science Foundation Grant GP 26633 and National Institutes of Health Grant RR 00711) for the use of the HXS 360-MHz facilities.

‡ Present address: Chemistry Department, University of Colorado, Boulder, CO 80303.

[1] Abbreviations used: NMR, nuclear magnetic resonance; EDTA, ethylenediaminetetraacetate; oligo(A), oligo(riboadenylic acid); oligo(U), oligo(ribouridylic acid); TSP, sodium 3-(trimethylsilyl)propionate-*2,2,3,3-d*$_4$.

0006-2960/81/0420-3986$01.25/0

& Hilbers (1977) observed the low-field imino proton region of oligo(A)-[oligo(U)]$_2$. They saw separate resonances for the Watson–Crick and reverse Hoogsteen base pairs. Kallenbach et al. (1976) observed similar results for other triplexes including AMP-[oligo(U_{15})]$_2$.

In this work, we report the ^{1}H NMR of oligonucleotides in a DNA duplex, an RNA duplex, a DNA–RNA hybrid duplex, and a DNA–RNA hybrid triplex, all of the same sequence. The molecules are (I) dCT_5G + dCA_5G, (II) rCU_5G + rCA_5G, (III) dCT_5G + rCA_5G, and (IV) rCU_5G + dCA_5G. The first three molecules form duplexes which all have different conformations in solution; IV forms (at least partially) a triple strand which is much less stable than the other structures. These results are consistent with optical studies previously reported on these molecules, where Job plots showed that I–III formed double-stranded complexes, whereas IV formed a triple-stranded structure (Martin & Tinoco, 1980).

The thermodynamics of oligonucleotides have been studied by optical methods (Martin et al., 1971) as well as by proton NMR. The T_m values of the helix-to-coil transition from both methods have agreed fairly well (Borer et al., 1975; Kallenbach et al., 1976; Patel, 1979). Melting of the end base pairs before the rest of the helix has been seen in several of the systems with A·U or A·T base pairs on the ends of the helix (Borer et al., 1975; Patel, 1975; Kallenbach et al., 1976). In helices with C·G base pairs on the ends, there seems to be no (Hughes et al., 1978) or little (Patel, 1979) differential melting of the ends of the helix before the rest of the oligonucleotide. However, most of the systems studied thus far have been self-complementary oligonucleotides [except for that of Hughes et al. (1978)]; this precludes measurement of the temperature dependence of the single strands. Ignorance of the temperature dependence of the single strand throughout the transition can lead to errors in the apparent T_m's; these errors will usually be larger for the interior base pairs than for the terminal ones. The oligonucleotides studied here are not self-complementary, so the single-strand dependences have been observed. The measured T_m for each base proton is thus a more accurate representation of the melting of that part of the helix.

Materials and Methods

The deoxyribooligonucleotides were synthesized by the diester method of Khorana (1968). The ribooligonucleotides were enzymatically prepared with polynucleotide phosphorylase (Martin et al., 1971; Uhlenbeck et al., 1971). Separation and purification of the oligomers were performed by RPC-5 column chromatography. Desalting of the samples was performed on Bio-Gel P-2 columns (Bio-Rad). All samples were run in 8.0 mM Na_2HPO_4, 20 mM NaH_2PO_4, 0.18 M NaCl, and 0.1 mM Na_2EDTA, pH 7.0, unless otherwise noted. Concentrations of the oligonucleotides were calculated from the absorbance of the solutions at 260 nm. The extinction coefficients were calculated from extinction coefficients of dinucleoside monophosphates and mononucleotides with the assumption of only nearest-neighbor interaction (Warshaw, 1965; Warshaw & Tinoco, 1966; Warshaw & Cantor, 1970). The values obtained in this way are 79×10^3, 58×10^3, 79×10^3, and 66×10^3 for dCA_5G, dCT_5G, rCA_5G, and rCU_5G, respectively, at 25 °C.

Experimental NMR. NMR spectra were taken on the HXS 360-MHz instrument at Stanford Magnetic Resonance Laboratory. Temperature was controlled to ±1 °C by a B-ST 100/700 Bruker temperature controller. Spectra of the nonexchangeable protons were measured in D_2O in the normal Fourier-transform mode with 5-mm NMR tubes (Wilmad). Spectra of the exchangeable protons were measured in H_2O with the Redfield 214 pulse sequence (Redfield et al., 1975) to minimize the water signal. For these samples, 5-mm microtubes which hold 160 μL of solution (508 CP Wilmad) were used. All solutions were measured at concentrations of either 1.0 or 0.5 mM per strand. Spectra measured in D_2O were all referenced to the internal standard TSP, while the spectra in H_2O were referenced to the H_2O peak. The temperature dependence of the chemical shift of H_2O relative to that of TSP was calibrated for our buffer. The chemical shifts obtained in this way are accurate to ±0.005 ppm for the D_2O and ±0.05 ppm for the H_2O studies. All data were collected with a Nicolet 1180 computer with 16K data points and a spectral width of ±1800 Hz for the D_2O work and 8K data points and a spectral width of ±5000 Hz for the H_2O. Spectra were taken every 10 °C from 35 to 65 °C and every 5 °C from 5 to 35 °C for the spectra in D_2O. In H_2O, measurements were made every 5 °C from 5 to 25 °C or until peaks were no longer observed.

D_2O samples were prepared by three lyophilizations against 99.8% D_2O (Bio-Rad) and then dissolved in 100% D_2O (Bio-Rad). The internal reference TSP was added to the sample after the addition of the 100% D_2O, since it had a tendency to remain insoluble after lyophilization with the oligonucleotides. Samples of the component oligomers titrated with Mn^{2+} were measured in D_2O with no buffer added at pD 7.0. The pD was calculated by adding 0.4 to the measured pH, with the pD adjusted by the addition of aqueous NaOD or DCl.

Results

Assignments of Nonexchangeable Protons. The assignments of the chemical shifts of the base protons were accomplished on the single strands. The method of incremental assignment was used at 65 °C where there is less stacking of the bases in the single strands (Borer et al., 1975). The chemical shifts at other temperatures were obtained from the change in peak position with temperature. Chemical shifts of the single-strand oligomers at 65 °C are given in Table I.

The aromatic region (6.6–8.5 ppm) of rCU_5G was poorly resolved due to the H6 doublets on the uracil residues, so no assignments were made in solutions which contained this oligomer. In the other solutions, the cytosine resonances were the only doublets in the aromatic region and were easily identified. The adenine H8 protons were differentiated from the adenine H2 protons because of the longer T_1 of the H_2 protons (Ts'o et al., 1973). The H8 on guanine was distinguished from H8 of adenine by the fact that it exchanges much faster upon heating in D_2O at 80 °C. In 1 h at 80 °C, the guanine H8 intensity was decreased over 50% while the adenine H2 intensity was decreased by about 10%.

In the oligonucleotide dCA_5G, we unambiguously assigned all the base protons on the cytosine, the guanine, and the adenine-2. Figure 1 shows the base proton spectrum of dCA_5G + dCT_5G in the single strands at 65 °C and also defines the numbering scheme. For the other ultimate adenine-6, we were able to specifically assign the H2, but not the H8, proton. The four H8 adenine resonances which belong to the three internal adenines (3–5) and adenine-6 were identified but not assigned to specific bases. The H2 protons on the three internal adenines all have very similar chemical shifts, and we were unable to assign resonances to particular adenines in the sequence.

In order to make assignment of the ultimate adenine resonances (2 and 6), it was necessary to study the smaller components of dCA_5G. The following compounds at 65 °C were used for comparison with dCA_5G (dCpApApApApG): dCpA, dCpApA, $dC(pA)_6$, dpApA, $d(pA)_4$, dpApG, and dpApApG.

Table I: Chemical Shifts (ppm) of Single Strands at 65 °C[a]

		C-1	A-2	A-3	A-4	A-5	A-6	G-7
dCA_5G	A H2		7.985	(7.752	7.725	7.696)	7.854	
	C H6	7.489						
	A or G H8		8.120	(8.081	8.052	8.016	8.012)	7.872
rCA_5G	A H2		8.091	(7.982	7.971	7.953)	8.034	
	C H6	7.632						
	A or G H8		8.265	(8.175	8.165	8.152)	8.190	7.878
		C-7	T-6	T-5	T-4	T-3	T-2	G-1
dCT_5G	C or T H6	7.770	7.532	7.627	7.627	7.627	7.645	
	T CH_3		1.878	1.878	1.878	1.878	1.878	
	G H8							7.993

[a] Spectra were taken on samples containing 8.0 mM Na_2HPO_4, 20 mM NaH_2PO_4, 0.18 M NaCl, and 0.1 mM Na_2EDTA, pD 7, at a concentration of 1 mM per strand. The values in parentheses indicated that we were unable to assign these peaks to particular bases in the sequence.

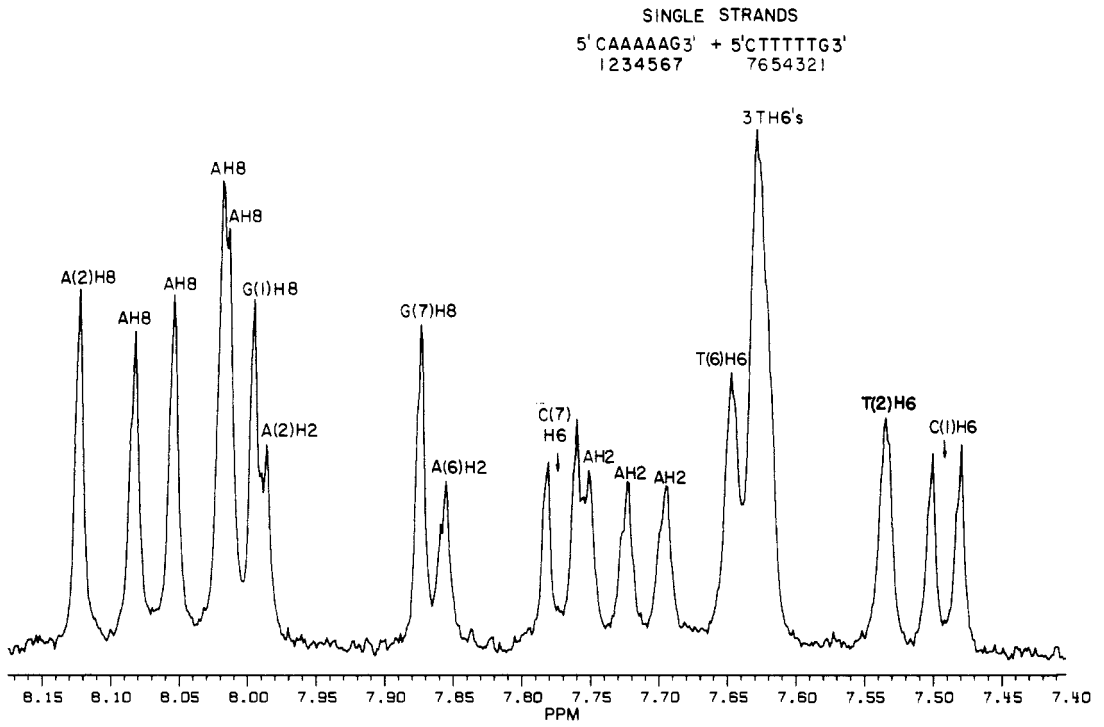

FIGURE 1: ^1H NMR (360-MHz) spectrum of the nonexchangeable base proton region of dCA_5G + dCT_5G in the single strands at 65 °C. The sample concentration was 1.0 mM per strand.

The assignments on the dCpA and dpApG were made by inspection. The assignment of the base protons in dpApA required studying their line widths when titrated with Mn^{2+}, which preferentially binds to the terminal phosphate at pD 7 and thus broadens the 5′ adenine protons relative to those of the 3′ adenine (Chiao & Krugh, 1977). This study enabled the assignments of the dpApA to be made, with both H8 protons unambiguously assigned and the two H2 protons only tentatively assigned; tentative assignment of the base protons on dApA has previously been made by Cheng & Sarma (1977). These assignments helped in the assignments of the dCpApA and dpApApG. Only partial assignments of the oligomers $dC(pA)_6$ and $d(pA)_4$ were possible. The chemical shifts of these component oligomers at 65 °C are published elsewhere (Pardi, 1980).

The assignments of the base protons in dCT_5G were made in a manner similar to that for dCA_5G. The components used were dCpT, dCpTpT, $dC(pT)_4$, and dpTpTpG. Unambiguous assignments of the cytosine and guanine base protons as well as the H6 protons on the ultimate thymines were made. The three internal thymine H6 protons all had the same chemical shifts at 65 °C. The assignments of the thymine methyl peaks to specific bases in the sequence were not made at any temperature.

Assignments of rCA_5G were made by comparison with the series $r(Ap)_nApG$ assigned by Shum (1977), as well as our analysis of the oligomers rCpA, rCpApA, and rCpApApApA. From this work, we were able to assign the cytosine and guanine base protons as well as the H8 and the H2 on the ultimate adenines. Again, the assignments of the three internal H8 protons or the three internal H2 protons to specific bases were not attempted.

The assignment of the base protons at other temperatures was made by following each peak shift with temperature; this is illustrated in Figures 2 and 3. Spectra were taken every 10 °C at higher temperatures, where there are small changes in chemical shifts with temperature, and every 5 °C in the range from 5 to 35 °C, where the peaks shift dramatically with temperature, and exchange broadening is evident. The assignment of the chemical shifts at 5 °C for the double-strand dCA_5G + dCT_5G was aided by comparison of spectra taken before and after the guanine H8 protons were exchanged in D_2O by heating at 75 °C for 1 h. Chemical shifts of this double strand are given in Table II. A small four-bond coupling of the thymine methyl protons with the H6 protons helps in the identification of H6 resonances. Assignment of the adenine H2 protons was aided by the fact that these peaks were sharper than the rest of the resonances in the double

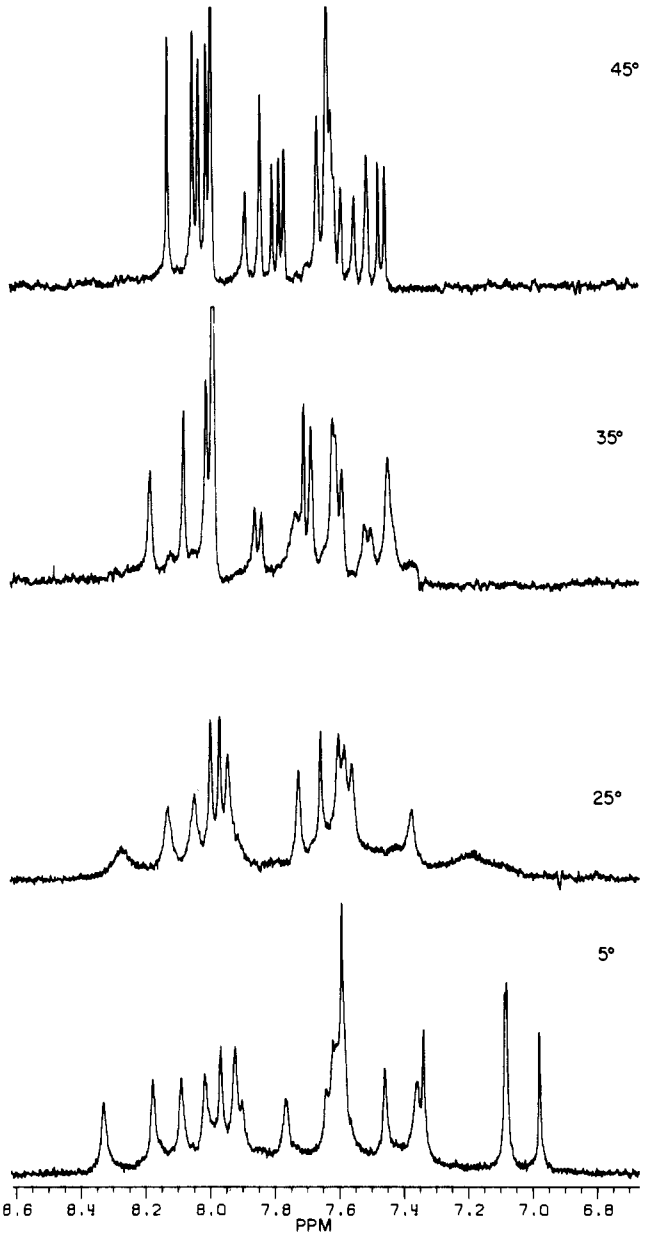

FIGURE 2: Temperature dependence of the nonexchangeable base protons in $dCA_5G + dCT_5G$. Sample concentration was 1.0 mM per strand.

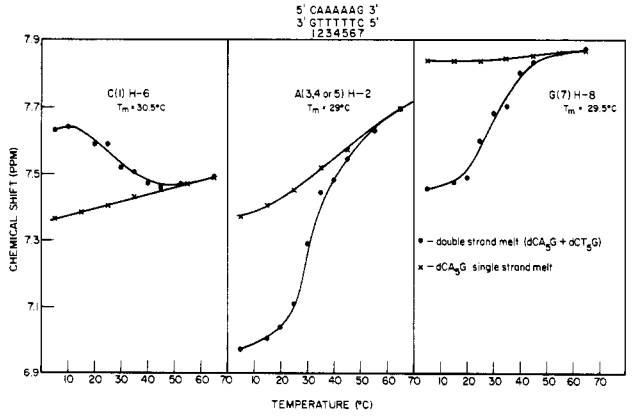

FIGURE 3: Melting curves (chemical shift vs. temperature) for the nonexchangeable base protons on $dCA_5G + dCT_5G$. The sample concentration was 1.0 mM per strand. The single-strand melt (×) and the double-strand melt (●) are shown.

strand, presumably because of their longer T_2 compared to the T_2 or the other protons. The base proton spectrum of $dCT_5G + dCA_5G$ in the double strand at 5 °C is shown in Figure 4.

The chemical shifts for the protons in the double-strand hybrid helix ($dCT_5G + rCA_5G$) which could be unambiguously followed are given in Table II. In the complexes $rCA_5G + rCU_5G$ and $rCU_5G + dCA_5G$, the spectra were so poorly resolved because of the uracil doublets that we were unable to see individual peaks in the aromatic region at temperatures lower than 35 °C.

The H1′ protons in deoxyribose and ribose sugars resonate at 5.5–6.5 ppm. The H1′ proton in deoxyribose sugars is coupled to the H2′ and H2″ protons while the ribose H1′ is only coupled to the H2′ proton. Thus, the H1′ protons on the two different rings are easily differentiated. We were not able to assign the H1′ protons to particular sugars in the sequence, but only to either deoxyribose or ribose sugars.

Assignment of the Base-Paired Imino Protons. The base-paired imino protons for the duplex $dCT_5G + dCA_5G$ are shown in Figure 5a. Partial assignment of these resonances was made by the temperature dependences of the protons, as well as by comparison with calculations of chemical shifts for the double strand. The guanine H1 proton involved in a hypothetical isolated base pair has been found to resonate 1 ppm upfield from the uracil or thymine H3 in the isolated base pair (Kearns & Shulman, 1974; Robillard & Reid, 1979). The numbers for these isolated base pairs derived from tRNA data are 14.4 ppm for the A·U base pair and 13.6 ppm for the C·G base pair (Robillard & Reid, 1979). Since there is only a limited amount of work available on the imino protons in deoxyribooligonucleotides of known sequence [see Sarma (1980), Chapters 5 and 6], the numbers for isolated base pairs derived from the tRNA work have been applied to the DNA helices.

For $dCA_5G + dCT_5G$ helix, the two resonances found at 12.93 and 13.55 ppm broaden before the other peaks. Figure 6 shows that at 20 °C these two peaks are extremely broad relative to the rest of the molecule, and by 25 °C they have disappeared. The differential broadening observed is due to the faster exchange of the terminal base-pair protons compared to those in the interior of the helix (Kan et al., 1975; Patel, 1975). Calculated chemical shifts of the two C·G resonances allow assignment of the resonance at 12.9 ppm to the C·G in the 1 position and the 13.55-ppm peak to the C·G in the 7 position (Arter & Schmidt, 1976) (see Table III). The assignments of the A·T base pairs were made by comparison with the calculated shifts for DNA B geometry and by comparison of the exchange rates of the imino protons with H_2O. The A·T resonance at 14.56 ppm had a shorter lifetime than the other A·T resonances (160 compared to 220 ms at 5 °C; Pardi, 1980), indicative of a penultimate base pair. Comparison of the calculated shifts of the penultimate base pairs allowed this resonance to be assigned to the 6 position. The rest of the A·T base pairs were assigned to the region 13.9–14.4 ppm.

In the $rCU_5G + rCA_5G$ system, we were aided in the assignments by comparison with the system $rCA_6 + rCU_5G$. (Data not shown, but see Figure 5b for the $rCA_5G + rCU_5G$ spectrum.) This gives unambiguous assignment of the C·G(1) base pair at 12.6 ppm, A·U(6) at 14.6 ppm, and C·G(7) at 13.6 ppm. The other resonances in the $rCU_5G + rCA_5G$ were assigned to the region 13.6–13.9 ppm. All chemical shifts at 5 °C are given in Table III.

In the duplex $rCA_5G + dCT_5G$, assignments were made in an analogous manner to the procedure used for the $dCA_5G + dCT_5G$ helix. The C·G resonances again show very different temperature dependences than the A·T protons. The ultimate

Table II: Experimental and Calculated Chemical Shifts (ppm) of the Nonexchangeable Base Protons in the Double Helix[a]

		1 $\vec{C}$ G $\leftarrow$	2 A T	3 A T	4 A T	5 A T	6 A T	7 G C
$dCA_5G + dCT_5G$ helix	A H2		7.337	(7.084	7.082	6.976)	7.590	
	C or T H6	7.630	7.356	(7.640	7.617	7.590)	7.760	7.910
	G or A H8	7.964	8.324	(8.173	8.085	8.012	7.920)	7.870
$rCA_5G + dCT_5G$ helix	A H2		7.766	(7.229	7.229	6.876)	7.317	
	C or T H6	*b*	7.860	(7.676	7.621	7.574)	7.502	~8.0
	G or A H8	*b*	8.163	*b*	*b*	*b*	*b*	*b*
calcn for DNA B form	A H2		6.78	6.92	6.99	7.07	7.73	
	C or T H6	7.93	7.83	7.84	7.84	7.85	7.83	7.94
	G or A H8	8.14	8.40	8.32	8.29	8.30	8.30	7.96
calcn for RNA A form	A H2		6.89	7.12	7.15	7.17	7.61	
	C or T H6	8.13	7.72	7.73	7.72	7.77	7.77	8.10
	G or A H8	8.05	8.46	7.89	7.83	7.83	7.80	7.98
calcn for RNA A′ form	A H2		6.80	7.06	6.82	6.89	7.57	
	C or T H6	8.13	7.71	7.72	7.71	7.76	7.76	8.10
	G or A H8	8.04	8.42	7.79	7.72	7.72	7.69	7.45

[a] Spectra were taken at 5 °C on samples containing 8.0 mM Na_2HPO_4, 20 mM NaH_2PO_4, 0.18 M NaCl, and 0.1 mM Na_2EDTA, pD 7.0, at a concentration of 1 mM per strand of $dCT_5G + dCA_5G$ and 0.5 mM per strand for $dCT_5G + rCA_5G$. The calculations were done by using numbers derived by Arter & Schmidt (1976), and we assumed thymine has the same ring current as uracil. The values in parentheses indicate that we were unable to assign these peaks to particular bases in the sequence (see text). [b] The poor resolution of the spectrum made assignment of this proton impossible at this temperature.

Table III: Experimental and Calculated Chemical Shifts (ppm) of the Imino Protons in the Double Helix[a]

	$\vec{C}$ G $\leftarrow$	A T	A T	A T	A T	A T	G C
$dCT_5G + dCA_5G$	12.94	(13.95	14.30	14.08	14.08)	14.56	13.51
$dCT_5G + rCA_5G$	12.38	13.40	(14.02	13.88	13.80)	14.53	13.52
$rCU_5G + rCA_5G$	12.52	(13.60	13.76	13.82	13.82)	14.60	13.60
DNA B-form calcn	12.53	13.50	13.80	13.80	13.85	14.15	13.30
RNA A-form calcn	12.80	13.46	13.70	13.70	13.70	14.10	13.50
RNA A′-form calcn	12.72	13.27	13.58	13.58	13.60	14.11	13.47

[a] Spectra were taken on solutions containing 8.0 mM Na_2HPO_4, 20 mM NaH_2PO_4, 0.18 NaCl, and 0.1 mM EDTA, pH 7.0, at a concentration of 1.0 mM per strand. The calculations were done by using numbers derived by Arter & Schmidt (1976), and we assumed thymine has the same ring current as uracil. The values in parentheses indicate that we were unable to assign these peaks to particular bases in the sequence.

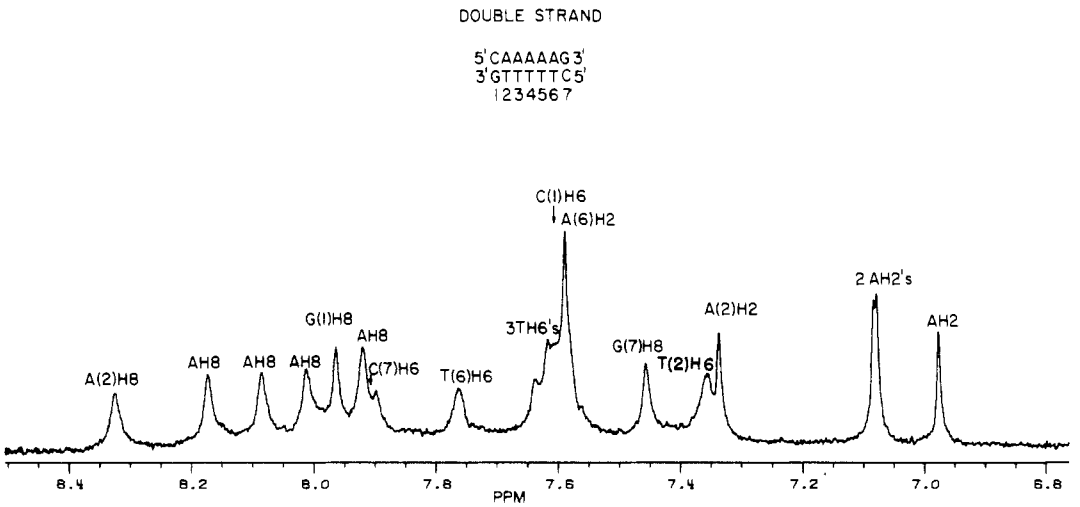

FIGURE 4: Assignments of the nonexchangeable base protons of $dCA_5G + dCT_5G$ in the double helix at 5 °C. The sample concentration was 1.0 mM per strand.

A·T base pairs show much shorter lifetimes for exchange of the imino protons than the interior A·T base pairs (Pardi, 1980). This information, along with comparison with the calculated chemical shifts (see Table III), allowed the terminal and penultimate base pairs to be assigned. The interior base pairs were then assigned to the region 13.7–14.0 ppm.

Temperature Dependence of the Nonexchangeable Protons in the Single Strands. The temperature dependence of the base protons of the single strands dCA_5G, dCT_5G, and rCA_5G has been studied. The cytosine H6 and H5, the adenine H2 and H8, the guanine H8, and the thymine H6 and methyl proton resonances were observed. The chemical shifts for all the base protons on dCT_5G show little change with temperature (<0.1 ppm from 5 to 65 °C). The largest changes are on the adenine H2 protons in dCA_5G and the adenine H8 protons on rCA_5G as shown in Figure 7. Most of the proton chemical-shift changes observed are not linear with temperature; this is important to note when analyzing melting curves,

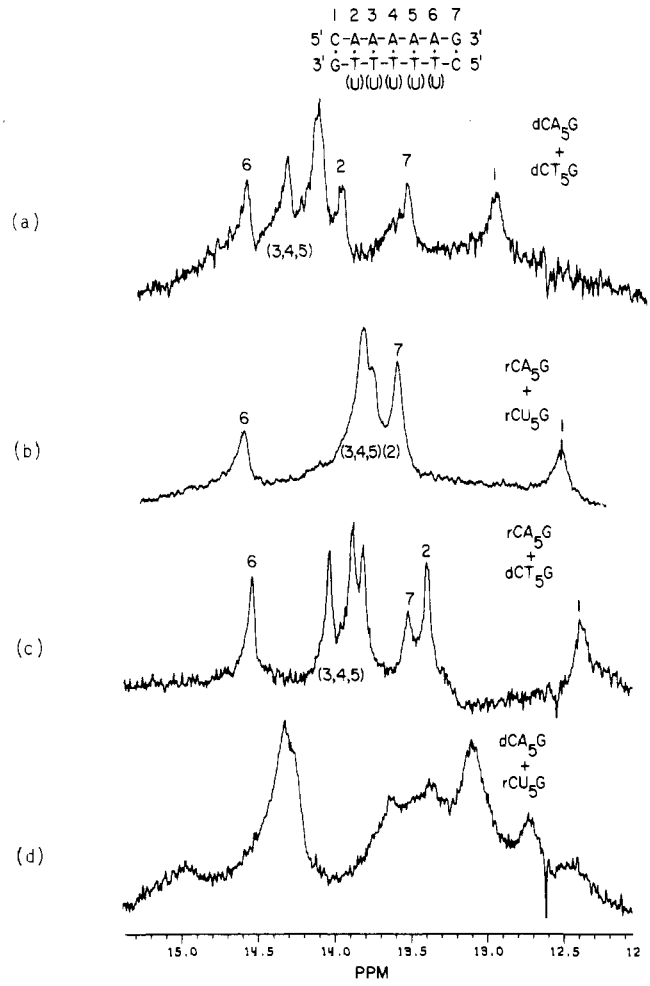

FIGURE 5: Comparison of the imino proton region of the four different helices: (a) $dCA_5G + dCT_5G$, (b) $rCA_5G + rCU_5G$, (c) $rCA_5G + dCT_5G$, and (d) $dCA_5G + rCU_5G$ at 5 °C. Spectra a–c were measured at concentrations of 1.0 mM per strand, whereas (d) was measured for a mixture of 1.0 mM dCA_5G plus 2.0 mM rCU_5G.

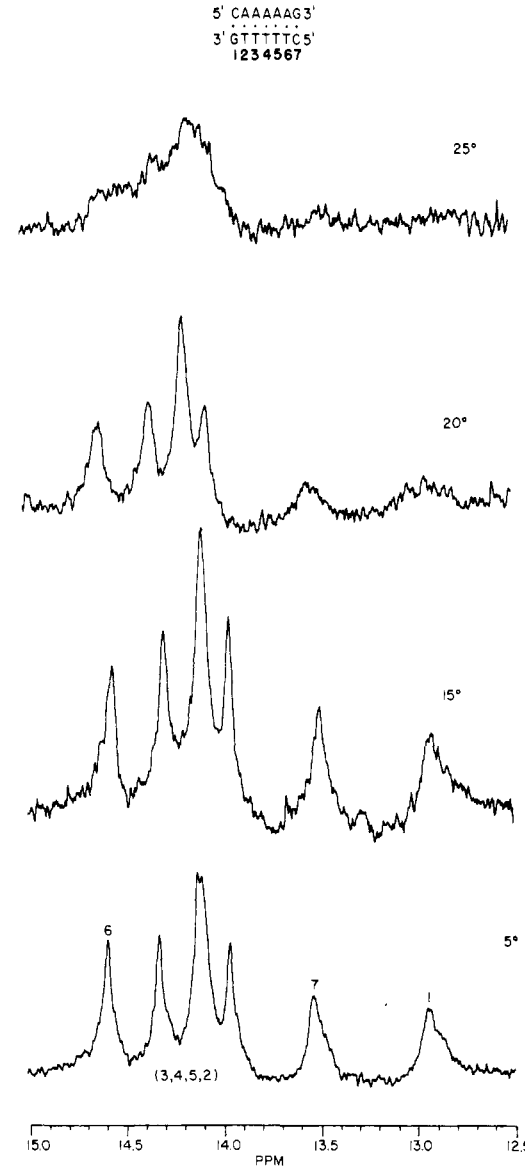

FIGURE 6: Temperature dependence of the imino protons in the $dCA_5G + dCT_5G$ double helix. The sample concentrations was 1.0 mM per strand.

as will be discussed in a later section. There are large differences in chemical-shift changes with temperature between dCA_5G and rCA_5G. The temperature dependences of the chemical shift for a particular proton are sometimes in opposite directions for the two strands. For example, compare the H6 of C (1) and the H8 of A (3, 4, 5, or 6) on the two strands in Figure 7. These observations indicate different conformations for the deoxyribose and ribose strands of CA_5G.

The best measures of base–base stacking from chemical shifts are obtained from the H2 of adenine and the H5 of the pyrimidines (Lee & Tinoco, 1980). The H8 of adenines and the H6 of pyrimidines have significant factors besides ring currents which affect their chemical shifts (Ts'o et al., 1969; Lee & Tinoco, 1980), such as the glycosidic torsion angle, the proximity of the sugar ring oxygens, or phosphate groups. Therefore, in order to get an idea of the relative base–base stacking in the dCA_5G and rCA_5G strands, we compared the chemical shifts of the adenine H2 protons. The adenine H2 protons on the ribose strand are always downfield (less shielded) from the same protons on the deoxyribose strand; this is indicative of more base–base stacking in dCA_5G than in rCA_5G.

Helix-to-Coil Transition of $dCT_5G + dCA_5G$ and $dCT_5G + rCA_5G$ As Followed by the Chemical Shift of the Base Protons. The temperature dependences of the chemical shifts of the base protons were studied in the oligonucleotides $dCT_5G + dCA_5G$ and $dCT_5G + rCA_5G$. In the helix-to-coil transition of $dCA_5G + dCT_5G$, all the base proton chemical shifts were followed from 5 to 65 °C. In the intermediate states from 20 to 35 °C, it is difficult to obtain exact chemical shifts of some of the protons due to extensive broadening of the resonances undergoing chemical exchange. In the other helix, $dCT_5G + rCA_5G$, the chemical exchange broadening over the 20–30 °C temperature range prevented the assignment of many of the resonances at lower temperatures. The chemical-shift changes with temperature for the deoxyribose helix are shown in Figure 3.

In order to monitor the helix-to-coil transitions in these oligomers, base protons were chosen which show large changes upon formation of the helical state (>0.1 ppm). The curves for many of these protons have sigmoidal shapes and characteristics which are very similar to absorbance vs. temperature curves for these oligomers. However, the NMR data allow one to follow the properties of individual bases throughout the double- to single-strand transition. Thus, NMR is more useful than absorbance studies for finding properties such as differential melting of the helix (Borer et al., 1975; Kan et al., 1975; Patel, 1975).

The melting temperatures, T_m's, of different bases were compared to learn if there is any melting on the ends of the

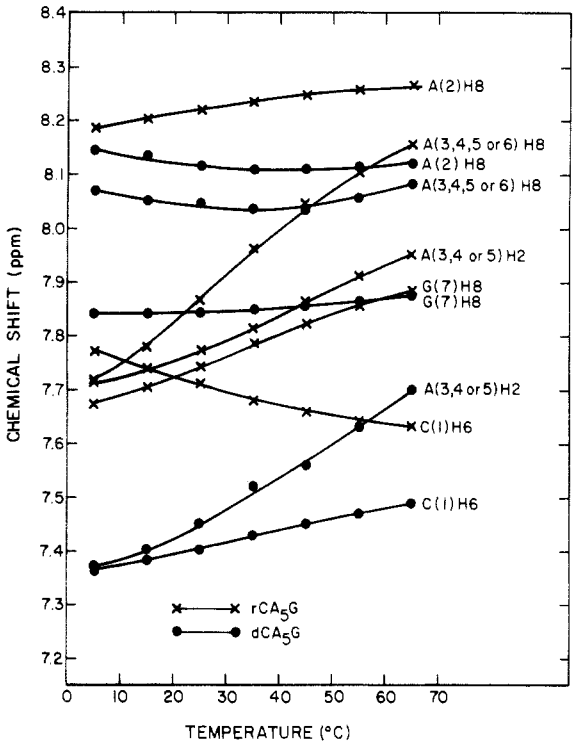

FIGURE 7: Comparison of the temperature dependences of the non-exchangeable base protons for rCA_5G (×) and dCA_5G (●) in the single strands.

dCT_5G + dCA_5G helix. The analysis was the same as that used in optical studies (Martin et al., 1971), which requires the melting behavior of the single strands. The single-strand molecule gives the upper base line in Figure 3, and the lower base line is the chemical shift measured at 5 °C. For most of the protons, there are very small chemical-shift changes between 5 and 15 °C so that the chemical shift of the double strand was taken to be temperature independent. The T_m values are all very similar for protons in different parts of the helix, with an average value of 29 ± 2 °C at a concentration of 1.0 mM per strand. Since all the base protons melt at approximately the same temperature, the concentration of partially formed helices is small.

Optical melting under identical conditions gives a T_m of 34 ± 2 °C. The difference is probably due to assumptions about the temperature dependence of the properties of the double strand and also errors involved in assuming fast exchange, on the NMR time scale, throughout the single- to double-strand transition. These effects will be discussed in a later section.

For the helix dCT_5G + rCA_5G, the temperature dependences of only some of the base protons were followed, since exchange broadening and overlap of too many protons hindered the identification of many of the protons in the double strand. In this helix, we were unable to follow any of the guanine or cytosine protons throughout the whole melting transition, so that it was not possible to tell if there was significant melting of the ends of the helix. The average T_m for all the base pairs was 23.5 °C at 0.5 mM per strand. The T_m obtained under similar conditions from optical data extrapolated to the same concentration was 25.7 °C (F. H. Martin, unpublished experiments).

The validity of T_m or enthalpy values extracted from melting curves is often dependent upon the method of analysis. In order to get useful results from a melting curve, one must estimate the temperature dependence of the measured property of the double- and single-stranded molecules (Martin et al., 1971). One major advantage in using non-self-complementary oligonucleotides is that the properties of the pure single strand can be studied separately from the double- to single-strand transition. The temperature dependence of the chemical shifts in the single strands often shows large deviations from linearity [see Figure 7 and Shum (1977)]. In self-complementary molecules, one is forced to assume linearity, which can lead to large errors in the T_m. For example, in the system dCA_5G + dCT_5G, the analysis of the melting curves with and without the experimental temperature dependence of the single strand gives T_m values which differ by up to 5 °C for some of the protons. This problem seems to be much more important in NMR than in optical studies, and should be taken into account when interpreting thermodynamic parameters derived from NMR melting curves.

Difficulties involved in obtaining equilibrium constants from chemical-shift data have recently been discussed (Feeney et al., 1979). One usually assumes that the system is always in fast exchange, on the NMR time scale, and that the measured chemical shift is a weight average of all the states. The validity of this approach breaks down when the system is not in the fast exchange domain, which happens during melting of most oligonucleotides. We have made calculations of the line shapes of the resonances for any exchange rates between two states, in order to estimate the errors made in extracting thermodynamic data with the assumption of fast exchange (Pardi, 1980). For parameters which reasonably mimic the behavior of the dCA_5G + dCT_5G system, we found that the system clearly is not in fast exchange throughout the helix-to-coil transition for many of the base protons. The effect of assuming fast exchange in our model system was to change the shape of the melting curve, especially below the T_m. The model calculations show that the assumption of fast exchange in analyzing experimental melting curves will lead to errors in drawing of the lower base line, and can give T_m values which are in error by up to 4–6 °C.

In the system dCA_5G + dCT_5G, the T_m found optically had a value ~5 °C higher than the T_m obtained by NMR, which showed all the resonances melting at 28–30 °C. We think the reason for this difference is the invalid assumption of fast exchange throughout the transition, which causes an incorrect estimation of the lower base line of the NMR melting curve. In these molecules, we took all the lower base lines to be flat, so that the error is probably systematic and will be similar for all the protons. Modeling this system gives the same conclusion, that the errors due to assuming fact exchange are approximately the same for all the protons. Therefore, we think that the terminal and interior base pairs melt at the same temperature, within 2–3 °C, and that an all-or-none transition is a good approximation for this duplex.

Temperature Dependence of the Exchangeable Imino Protons. The temperature dependence of the imino base protons in dCT_5G + dCA_5G is shown in Figure 6. As already discussed in the section on the assignments of the imino protons, it is found that the base pairs on the ends broaden and disappear before the rest of the base pairs in the helix. Similar broadening is observed for the other helices, dCT_5G + rCA_5G and rCU_5G + rCA_5G (Pardi, 1980). The broadening phenomenon observed is due to chemical exchange (Gutowsky & Holm, 1956; Kaplan & Fraenkel, 1980), as will be discussed in a later section. The C·G imino protons for the three systems broaden and disappear in the range from 17 to 23 °C. There is little chemical-shift change with temperature for any of these resonances. Differences in the extent of broadening for a particular proton at a given temperature are seen in the three systems; this is due to different lifetimes for exchange of the

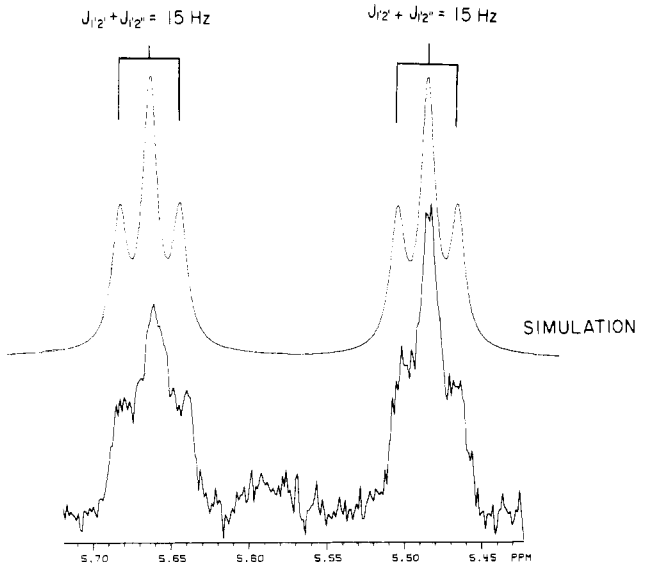

FIGURE 8: H1′ proton spectrum for two sugar residues in double-stranded $dCA_5G + dCT_5G$ at 5 °C is shown along with its computer simulation. Only these H1′ protons were resolvable from the bulk of the sugar resonances (see text). The best fit to the simulation was for $J_{1',2'} + J_{1',2''} = 15 \pm 1$ Hz.

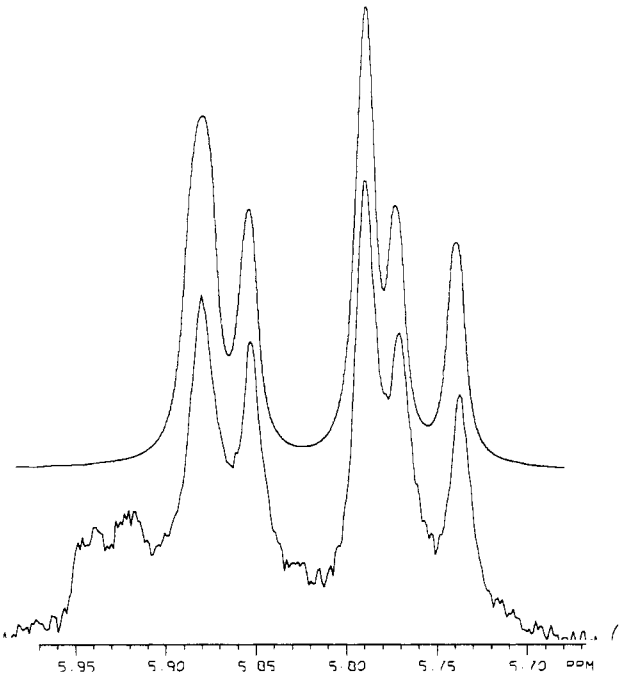

FIGURE 9: Seven ribose H1′ protons are shown for double-stranded $rCA_5G + dCT_5G$ at 5 °C (bottom) along with their simulation (top). The CH5 base proton from the dCT_5G strand is seen at 5.93 ppm in the experimental spectrum. The simulation was done for the H1′ ribose protons from the rCA_5G strand in the double strand. The best fit for all the $J_{1',2'}$ coupling constants was less than or equal to 1.5 Hz.

imino protons with H_2O. We are investigating the lifetimes of the imino protons in these systems by the saturation recovery method used by Redfield (Johnston & Redfield, 1978). Preliminary results on the $dCA_5G + dCT_5G$ helix show that the lifetimes of the terminal C·G base-paired protons are between 15 and 50 ms, and that the lifetimes of the internal protons range from 150 to 250 ms at 5 °C (Pardi, 1980).

Sugar Pucker of the Furanose Ring in the Double Strand. In two of the oligomer systems, the sugar pucker for some of the ribose or deoxyribose rings were calculated. The conformation of the ribose or deoxyribose ring has been described by Altona & Sundaralingam (1973) as a two-state equilibrium between type N (C2′ exo, C3′ endo) and type S (C2′ endo, C3′ exo). The ribose ring conformation can then be calculated from the fact that in the N-type conformation $J_{1',2'} = \sim 0$ Hz, and the S type has $J_{1',2'} = \sim 10$ Hz. For the deoxyribose ring, the N-type conformation has the property of $J_{1',2'} + J_{1',2''} = \sim 7$ Hz while the S type has a value of ~ 16 Hz for this sum (Altona & Sundaralingam, 1973).

The assignment of the H1′ protons to particular sugars in the oligomers was not possible, and coupling constants were obtained only for those resonances which were well separated from the main group of H1′ protons. For the $dCA_5G + dCT_5G$ helix at 5 °C, only two H1′ deoxyribose protons at 5.64 and 5.48 ppm were separated from the rest. Both protons had coupling constants of $J_{1',2'} + J_{1',2''} = 15 \pm 1$ Hz (see Figure 8), which gives 90% S-type (2′ endo) conformation for these sugars. The temperature dependence of these peaks, as well as comparison with the single strands at 65 °C, shows that both protons are from the dCA_5G strand. The fact that these deoxyribose sugars are in 90% S-type (2′ endo) conformation is consistent with a B-family geometry for at least part of this helix.

In the hybrid oligonucleotides $rCA_5G + dCT_5G$, all seven ribose H1′ protons were resolved and had coupling constants $J_{1',2'} \leq 1.5$ Hz, as seen in Figure 9. The ribose ring sugar pucker is then calculated to be ≥85% N-type (3′ endo) conformation. This 3′-endo sugar pucker in the ribose strand of the double helix is indicative of an A-family geometry for the helix.

Line Widths of the Base Protons and Chemical Exchange. For the $dCA_5G + dCT_5G$ system, we see extensive broadening of some of the base protons during the melting transition. The fact that some of the resonances broaden while others stay very sharp is clearly seen in Figure 2. The reason for this broadening is the fact that the system is undergoing chemical exchange between the double-stranded helix (helix) and the single strands (coil). The rate of exchange and the population difference as well as the difference in chemical shift between the two states are the factors which lead to broadening of the resonances (Gutowsky & Holm, 1956). Resonances such as the guanine-1 H8 at 7.95 ppm and the thymines (3–5) H6 at ~7.6 ppm all shift little and therefore are sharp throughout the transition. The three interior adenine H2 protons (at 7.09, 7.08, and 6.98 ppm at 5 °C) have such large chemical-shift differences for the two states that their resonances are almost broadened into the base line at 25 °C.

The adenine-2 H8 proton (8.32 ppm at 5 °C) is well separated from its neighbors and broadens to a moderate extent, which makes it possible to extract constants for the helix-to-coil transition (Patel, 1975, 1979). Equation 1 applies when the

$$\frac{1}{\pi T_2(\text{obsd})} = \frac{P_C}{\pi T_2(C)} + \frac{P_H}{\pi T_2(H)} + 4\pi P_C^2 P_H^2 (\nu_H - \nu_C)^2 (\tau_H + \tau_C) \quad (1)$$

system is close to the fast exchange limit (Kaplan & Fraenkel, 1980) and has been used to calculate rate constants for the helix-to-coil transitions in other oligonucleotides (Patel, 1975, 1979). $1/[\pi T_2(H)]$ and $1/[\pi T_2(C)]$ are the measured line widths of the helix and coil states, respectively, while $1/[\pi T_2(\text{obsd})]$ is the observed line width in the broadened spectrum. The line width of the helix state for a particular proton is assumed to be independent of temperature and is thus the measured line width of the helix at 5 °C. The line width of the coil was taken from the measured line width during the

melting of the single strand. ν_H and ν_C are chemical shifts of the protons in the helix and coil given in hertz, again, ν_H is assumed to be the chemical shift of the helix at 5 °C, while ν_C is measured from the melting of the single strand. P_H and P_C are the populations at a given temperature for the double and single strands, respectively. The populations were obtained from analysis of the absorbance vs. temperature melting curve. τ_H and τ_C are the lifetimes of the helix and coil states; by the definitions, $P_H\tau_C = P_C\tau_H$. At 25 °C for the $dCA_5G + dCT_5G$ helix and the adenine-2 H8 proton, the following parameters were obtained: $1/[\pi T_2(H)] = 6$ Hz, $1/[\pi T_2(C)] = 2$ Hz, $P_H = 0.88$, $P_C = 0.12$, $1/[\pi T_2(obsd)] = 15$ Hz, and $\nu_H - \nu_C = 72$ Hz. Using eq 1, we calculate the lifetimes to be $\tau_H = 14$ ms and $\tau_C = 2$ ms. Since the measurements of these lifetimes are fairly indirect, the errors in the numbers are of the order of 30–40%. These lifetimes and their rate constants are consistent with kinetic results obtained on other oligonucleotides by temperature jump methods (Porschke & Eigen, 1971; Ravetch et al., 1973).

Discussion

Comparison of the Structures of Oligonucleotide Complexes in Solution. The Double-Stranded Structures. Figure 5a–c shows low-field spectra of the three double-stranded helices at 5 °C. There are seven imino protons in each spectrum, one for each base pair in the double helix. From examining the chemical shifts of the imino protons in the three double strands, one sees distinct differences in the peak positions of many protons. This is indicative of different conformations for each system.

RNA structures are found to be less susceptible to conformational changes than their DNA counterparts (Arnott et al., 1975). We would then expect that the RNA helix in our study would be close to RNA A-form geometry. As seen in Table III, there are large differences between the experimental results and the calculations of the chemical shifts for an RNA A or A′ geometry. These differences can be due to several factors, such as inaccurate values for the ring currents used in the calculations, incorrect geometries assumed in the calculations, sequence-dependent geometries, or other parameters besides ring currents having significant effects on the chemical shifts of the imino protons [see Borer et al. (1975) for a discussion of these effects]. Aggregation will also directly affect the chemical shifts of the terminal base-pair protons. Optical studies on these oligonucleotides have shown that there is significant aggregation at these concentrations, so the chemical shifts from the terminal base pairs are more difficult to interpret.

The chemical shifts of the nonexchangeable base protons are compared with the calculated results for several of the oligonucleotide double helices in Table II. One sees large discrepancies between the experimental and calculated chemical shifts for the $dCA_5G + dCT_5G$ system. We are investigating the discrepancies to see if the differences are due to the oligonucleotide being in a slightly different geometry than the classical DNA B form. Calculations of the chemical shifts for other energy-minimized geometries are presently being performed to see how slight changes in helical parameters, such as winding angle, twist, and tilt, affect the chemical shifts of the base protons.

The coupling constants and chemical shifts of the ribose and deoxyribose protons have been extensively used in the past to obtain conformational information on oligonucleotides in solution (Lee et al., 1976; Ezra et al., 1977). One of the most meaningful parameters in the geometry of the nucleic acid is the conformation of the sugar ring (Arnott & Hukins, 1973). In the $dCT_5G + dCA_5G$ double helix, two of the deoxyribose sugar rings in the dCA_5G strand were found to be 90% in a 2′-endo conformation. The 2′-endo sugar puckers are found in B-form geometries, which is consistent with this helix being in a B-family conformation.

The hybrid $dCT_5G + rCA_5G$ was also well-enough resolved in the H1′ proton region to obtain coupling constant data. The evidence of a 3′-endo conformation of the ribose strand is indicative of an A-family geometry. Knowing the sugar pucker of the helix greatly restricts the range of conformations for the sugar phosphate backbone, thereby ruling out many possible geometries for the helix.

Triple Strand. The system $rCU_5G + dCA_5G$ has been shown to form a triple strand under our conditions (Martin & Tinoco, 1980). The low-field imino proton spectrum of this mixture is quite different than the other spectra shown in Figure 5. For example, there is a broad resonance at very low field around 15.0 ppm in Figure 5d, and the normal Watson–Crick imino protons are not found to resonate higher than ~14.6 ppm. This resonance as well as those centered at 14.6 ppm is most likely due to reverse Hoogsteen base pairs involved in the triple strand.

Geerdes & Hilbers (1977) have studied oligo(A)-[oligo(U)]$_2$ triplexes in solution by ^{1}H NMR. From the chemical shifts of the imino protons, they proposed ~14.3 ppm for the intrinsic position of the Watson–Crick A·U pair in the triple strand and 14.8 ppm for the reverse Hoogsteen pair. Robillard & Reid (1979) have recently attempted calculations which empirically optimize the magnitudes of the chemical shifts of the isolated base pairs by a method which assumes a strong similarity between the crystal and solution structures of tRNA. They found the optimized intrinsic position of the reversed Hoogsteen A·U to be at 14.9 ppm. Kallenbach et al. (1976) have studied triple-stranded structures in which oligo(U_{15}) and rAMP showed two sets of imino resonances, presumably one for the Watson–Crick and one for the reverse Hoogsteen base pairs. They concluded that the most probable intrinsic chemical shift was 14.1 ppm for the reverse Hoogsteen base pair but were unable to rule out an alternate assignment in which the intrinsic chemical shift was ~14.8 ppm.

In our system, we are unable to make unambiguous assignments of the imino protons, but we think that the broad resonance at ~15.0 ppm is due to an A·U reverse Hoogsteen base pair. It seems to resonate at too low field to be from a normal Watson-Crick-type A·U resonance, and the above studies on triplexes indicate that the reverse Hoogsteen base pair's intrinsic shift may be in the region of 15.0 ppm. This would indicate that the other resonances at 14.2–14.5 ppm would also be mostly from Hoogsteen base pairs. The resonances below 14.0 ppm are then due to Watson–Crick-type base pairs. The intrinsic shift of an rU·dA·rU reverse Hoogsteen pair would then be ≥15.0 ppm.

The fact that there are so many types of resonances in the low-field region of the $dCA_5G + rCU_5G$ system, many more than the seven protons one sees in the double-helical systems, indicates that the oligomers are fully or partially in the triple-strand conformation.

Fraying vs. Melting of Oligonucleotides. It is important to understand the distinction between fraying of the ends and the differential melting of the ends of an oligonucleotide. Here, we define the melting of a base pair in the oligomer with respect to the fraction of the base pair which is formed, or involved in hydrogen bonding. An 80% melted base pair would have an equilibrium concentration of oligonucleotides with 80% of that base pair broken and 20% of that base pair formed.

Melting thus reflects an equilibrium effect and is dependent only upon the concentrations of the two states.

Fraying is defined as the rapid opening and closing of a base pair (Patel & Hilbers, 1975; Hilbers, 1979). It is thus a kinetic effect, and the important parameters involved are the rate constants linking the open and closed states. Fraying can mainfest itself in the H-bonding imino protons where the exchange rate of the proton is reflected by the line width of the resonance [see Crothers et al. (1974) and Hilbers (1979) for a discussion of the exchange of imino protons with H_2O]. In our oligomer systems, the C·G base-paired imino protons broaden and disappear before the interior base pairs, which is indicative of fraying of the ends of the helix. This does not mean the end base pairs are melted at the point where the resonance has disappeared. For example, in the helix dCT_5G + dCA_5G at 25 °C, the imino proton region is extremely broad, and by 30 °C the resonances have disappeared into the base line (see Figure 6). This is not representative of the equilibrium concentrations of these states; the oligomer is fraying at this point, but it is not melted. In fact, the chemical shift vs. temperature data of protons on all bases, and optical studies of this oligomer, show that it is >50% in the double strand at 30 °C, where all the imino protons have disappeared. The temperature dependence of the broadening of the imino protons is mainly a kinetic, not an equilibrium, effect. Thus, an end base pair can be fraying but not "melted" at the same time. In our system, although we see fraying of the ends of the helix, i.e., the end bases are opening and closing faster than the interior base pairs, the ends do not melt appreciably lower than the rest of the helix. It is worth noting that not only do fraying and melting reflect different processes but also there may be different states involved in the two processes. For example, in order for an imino proton to exchange with water, the base pair must open to some extent. This open state most likely differs from the "melted" state in a molecule with differential melting on the ends of the helix. Care should be taken in distinguishing between fraying and melting, as well as the effects ascribed to them.

Conclusions

We have studied the following oligonucleotides separately and in their complementary mixtures by proton NMR: dCA_5G, dCT_5G, rCA_5G, and rCU_5G. Results on the single strands show that the ribose and deoxyribose strands of Ca_5G have different conformations in solution, and specifically that there is more base–base stacking in the deoxyribose strand.

Results on the mixtures indicate that rCU_5G + dCA_5G at least partially forms a triple strand with a 2:1 rCU_5G:dCA_5G helix, while rCU_5G + rCA_5G, rCA_5G + dCT_5G, and dCT_5G + dCA_5G form double-helical structures. Comparison of the three double strands shows that they all have different structures in solution. The sugar ring pucker in these systems indicates that the deoxyribose helix (dCA_5G + dCT_5G) is in a B-family geometry, whereas the hybrid helix (rCA_5G + dCT_5G) is in an A-family geometry.

The melting of the helix dCA_5G + dCT_5G as followed by the chemical-shift changes of the nonexchangeable base protons shows that base pairs on the ends of the helix melt at approximately the same temperature as that for the interior base pairs. The temperature dependence of the imino protons indicates there is fraying of the ends of the helix. Thus, this helix exhibits fraying of the ends, but very low concentrations of partially formed helices at the same time. These results indicate that a two-state model is a good approximation of the helix-to-coil transition in this oligonucleotide, as often assumed in optical studies. Some of the biological implications due to the differences in stability of these oligonucleotides have been discussed elsewhere (Martin & Tinoco, 1980). The differing conformations for these DNA, RNA, and hybrid helices may also be important in enzymatic recognition of different types of helices.

Studies on the kinetics of these oligonucleotide helices, as well as the changes in the conformation and stability of double-helical oligonucleotides when there is a mismatched base on one strand, or when frameshift mutagens are bound, are presently being pursued.

Acknowledgments

We thank David Koh and Barbara Dengler for help in synthesis of oligonucleotides and Kathleen Morden for help in data acquisition.

References

Altona, C., & Sundaralingam, M. (1973) *J. Am. Chem. Soc. 95*, 2333–2345.

Arnott, S., & Hukins, D. W. L. (1973) *J. Mol. Biol. 81*, 93–105.

Arnott, S., Chandrasekaran, R., & Selsing, E. (1975) in *Structure and Conformations of Nucleic Acids and Protein-Nucleic Acid Interactions* (Sundaralingam, M., Ed.) pp 577–596, University Park Press, Baltimore, MD.

Arter, D. B., & Schmidt, P. G. (1976) *Nucleic Acids Res. 3*, 1437–1447.

Arter, D. B., Walker, G. C., Uhlenbeck, O. C., & Schmidt, P. G. (1974) *Biochem. Biophys. Res. Commun. 61*, 1089–1094.

Bloomfield, V. A., Crothers, D. M., & Tinoco, I., Jr. (1974) *Physical Chemistry of Nucleic Acids*, pp 339–342, Harper and Row, New York.

Borer, P. N., Kan, L. S., & Ts'o, P. O. P. (1975) *Biochemistry 14*, 4847–4863.

Cheng, D. M., & Sarma, R. H. (1977) *J. Am. Chem. Soc. 99*, 7333–7348.

Chiao, Y. C. C., & Krugh, T. R. (1977) *Biochemistry 16*, 747–755.

Cross, A. D., & Crothers, D. M. (1971) *Biochemistry 10*, 4015–4023.

Crothers, D. M., Cole, P. E., Hilbers, C. W., & Shulman, R. G. (1974) *J. Mol. Biol. 87*, 63–88.

Early, T. A., Kearns, D. R., Burd, J. F., Larson, J. E., & Wells, R. D. (1977) *Biochemistry 16*, 541–551.

Ezra, F. S., Lee, C. H., Kondo, N. S., Danyluk, S. S., & Sarma, R. H. (1977) *Biochemistry 16*, 1977–1987.

Feeney, J., Batchelor, J. G., Albrand, J. P., & Roberts, G. C. K. (1979) *J. Magn. Reson. 33*, 519–529.

Geerdes, H. A. M., & Hilbers, C. W. (1977) *Nucleic Acids Res. 4*, 207–221.

Gutowsky, H. S., & Holm, C. H. (1956) *J. Chem. Phys. 25*, 1228–1234.

Heller, M. J., Anthony, T. T., & Maciel, G. E. (1974) *Biochemistry 13*, 1623–1631.

Hilbers, C. W. (1979) in *Biological Applications of Magnetic Resonance* (Shulman, R. G., Ed.) pp 1–44, Academic Press, New York.

Hughes, D. W., Bell, R. A., England, T. E., & Neilson, T. (1978) *Can. J. Chem. 56*, 2243–2248.

Johnston, P. D., & Redfield, A. G. (1978) *Nucleic Acids Res. 5*, 3913–3927.

Kallenbach, N. R., Daniel, W. E., Jr., & Kaminker, M. A. (1976) *Biochemistry 15*, 1218–1223.

Kan, L. S., Borer, P. N., & Ts'o, P. O. P. (1975) *Biochemistry 14*, 4864–4869.

Kaplan, J. I., & Fraenkel, G. (1980) *NMR of Chemically Exchanging Systems*, pp 74-80, Academic Press, New York.
Kearns, D. R., & Shulman, R. G. (1974) *Acc. Chem. Res. 7*, 33-39.
Khorana, H. G. (1968) *Pure Appl. Chem. 17*, 349-381.
Lee, C. H., & Tinoco, I., Jr. (1980) *Biophys. Chem. 11*, 283-294.
Lee, C. H., Ezra, F. S., Kondo, N. S., Sarma, R. H., & Danyluk, S. S. (1976) *Biochemistry 15*, 3627-3638.
Martin, F. H., & Tinoco, I., Jr. (1980) *Nucleic Acids Res. 8*, 2295-2299.
Martin, F. H., Uhlenbeck, O. C., & Doty, P. (1971) *J. Mol. Biol. 57*, 201-215.
Milman, G., Langridge, R., & Chamberlin, M. J. (1967) *Proc. Natl. Acad. Sci. U.S.A. 57*, 1804-1810.
Pardi, A. (1980) Ph.D. Thesis, University of California, Berkeley.
Patel, D. J. (1974) *Biochemistry 13*, 2396-2402.
Patel. D. J. (1975) *Biochemistry 14*, 3984-3989.
Patel, D. J. (1979) *Eur. J. Biochem. 96*, 267-276.
Patel, D. J., & Hilbers, C. W. (1975) *Biochemistry 14*, 2651-2656.
Porschke, D., & Eigen, M. (1971) *J. Mol. Biol. 62*, 361-381.
Ravetch, J., Gralla, J., & Crothers, D. M. (1973) *Nucleic Acids Res. 1*, 109-127.
Redfield, A. G., Kunz, S. D., & Ralph, E. K (1975) *J. Magn. Reson. 19*, 114-117.
Robillard, G. T., & Reid, B. R. (1979) in *Biological Applications of Magnetic Resonance* (Shulman, R. G., Ed.) pp 45-112, Academic Press, New York.
Sarma, R. H. (1980) *Nucleic Acid and Geometry and Dynamics*, Pergamon Press, New York.
Selsing, E., Wells, R. D., Early, T. A., & Kearns, D. R. (1978) *Nature (London) 21*, 249-250.
Shum, B. W. K. (1977) Ph.D. Thesis, Yale University.
Ts'o, P. O. P., Kondo, N. S., Schweizer, M. P., & Hollis, D. P. (1969) *Biochemistry 8*, 997-1029.
Ts'o, P. O. P., Barrett, J. C., Kan, L. S., & Miller, P. S. (1973) *Ann. N.Y. Acad. Sci. 222*, 290-306.
Uhlenbeck, O. C., Martin, F. H., & Doty, P. (1971) *J. Mol. Biol. 57*, 217-229.
Warshaw, M. M. (1965) Ph.D. Thesis, University of California, Berkeley.
Washaw, M. M., & Tinoco, I., Jr. (1966) *J. Mol. Biol. 20*, 29-38.
Warshaw, M. M., & Cantor, C. R. (1970) *Biopolymers 9*, 1079-1103.

Study of Transfer Ribonucleic Acid Unfolding by Dynamic Nuclear Magnetic Resonance†

Paul D. Johnston‡ and Alfred G. Redfield*

ABSTRACT: Nuclear magnetic resonance (NMR) measurements of proton exchange were performed on yeast $tRNA^{Phe}$, and in much less detail on *Escherichia coli* $tRNA^{fMet}$, over a range of Mg^{2+} concentrations and temperatures, at neutral pH and 0.1 M NaCl. The resonances studied were those of ring nitrogen protons, resonating between 10 and 15 ppm downfield from sodium 3-(trimethylsilyl)-1-propanesulfonate, which partake in hydrogen bonding between bases of secondary and tertiary pairs. Methods include saturation-recovery, line width, and real-time observation after a change to deuterated solvent. The relevant theory is briefly reviewed. We believe that most of the higher temperature rates reflect major unfolding of the molecule. For *E. coli* $tRNA^{fMet}$, the temperature dependence of the rate for the U8-A14 resonance maps well onto previous optical T-jump studies for a transition assigned to tertiary melting. For yeast $tRNA^{Phe}$, exchange rates of several resolved protons could be studied from 30 to 45 °C in zero Mg^{2+} concentration and had activation energies on the order of 40 kcal/mol. Initially, the tertiary structure melts, followed shortly by the acceptor stem. At high Mg^{2+} concentration, relatively few exchange rates are measurable below the general cooperative melt at about 60 °C; these are attributed to tertiary changes. Real-time observations suggest a change in the exchange mechanism at room temperature with a lower activation energy. The results are compared with those obtained by other methods directed toward assaying ribonucleic acid dynamics.

Knowledge of the modes of flexibility of transfer ribonucleic acid (tRNA) is interesting in itself and is relevant to other RNA classes. The rates of exchange with solvent of labile protons within tRNA are likely to reflect such flexibility. Nuclear magnetic resonance (NMR) provides a potentially powerful way to study exchange rates, provided that resonances can be identified. The present paper summarizes our measurements of such rates as a function of temperature and magnesium concentration, and their interpretation in light of recent studies directed toward identification (Johnston & Redfield, 1981).

Physical studies of tRNA have been reviewed by Crothers & Cole (1978) and Crothers (1979). There is good evidence that in the presence of 0.1 M NaCl, as used in our work, the structure of tRNA approximates the native, active form whether magnesium is present or not. In the presence of magnesium, the native structure is stable to fairly high tem-

† From the Department of Biochemistry, Brandeis University, Waltham, Massachusetts 02254. *Received January 12, 1981.* This work was supported in part by U.S. Public Health Service Grants GM20168 and 5T01-GM0212 and by the Research Corporation. This is Publication No. 1368 of the Brandeis University Biochemistry Department. A.G.R. is also at the Physics Department and the Rosensteil Basic Medical Sciences Research Center of Brandeis University.

‡ Present address: Institute of Molecular Biology, University of Oregon, Eugene, OR 97403.

0006-2960/81/0420-3996$01.25/0